JOURNAL OF CATALYSIS **171,** 398–405 (1997)
ARTICLE NO. CA971835

Ligand and Geometric Effects on Pt/Nb_2O_5 and $Pt–Sn/Nb_2O_5$ Catalysts

Donato A. G. Aranda and Martin Schmal[1]

NUCAT/COPPE-PEQ/UFRJ, Federal University of Rio de Janeiro, Brazil-Caixa Postal 68502; CEP : 21945-970 Rio de Janeiro, Brazil

Received July 22, 1996; revised July 21, 1997; accepted July 23, 1997

Pt and Pt–Sn catalysts supported on alumina and niobia were prepared to investigate the geometric and ligand effects by thermal desorption and infrared of CO adsorption, as well as by studying their catalytic activity and selectivity for 1,3-butadiene hydrogenation. Results have shown a significant increase in the platinum electronic density on Pt/Nb_2O_5 catalysts caused by the SMSI effect. $Pt–Sn/Nb_2O_5$ catalysts have shown alteration of electronic density after reduction at higher temperatures due to alloying of Pt–Sn on niobia surface. Results obtained in the metallic phase for the alumina supported catalysts could be successfully explained by ensemble effect. Both niobia and alumina surfaces seem to participate in CO adsorption/desorption process through formate species and carbon monoxide plus hydroxyl reactions.

INTRODUCTION

Bimetallic catalysts consisting of Pt as the primary metal and an inactive second metal such as Sn dispersed on alumina are commonly used in nafta reforming industry (1, 2). Recently, interest in the dehydrogenation processes has increased due to the high demand for the production of oxygenated compounds in reformulated gasoline and C_9–C_{14} mono-olefins to obtain biodegradable detergents (3, 4). These processes have been performed with Pt–Sn catalysts. The mechanism of the promoting effect of these bimetallic catalysts is still a controversial issue in the literature (5–7). In summary, the ensemble effect, which is caused by the dilution of platinum particles in the presence of tin, and the ligand effect, which is related to changes in the electronic density of the metals, explain the stability and selectivity of these catalysts.

The Pt/Nb_2O_5 and $Pt–Sn/Nb_2O_5$ catalysts are excellent catalysts, which exhibit high selectivities for the dehydrogenation reactions (8–10). The promoting effect on niobia is more complex than on $Pt–Sn/Al_2O_3$. On niobia, both the metals and the SMSI effect are important and require additional experiments to explain the promoting mechanism.

In this work, we studied the influence of the promoting effect of Pt–Sn supported on niobia and the nature of the electronic and geometric effects, by using infrared spectroscopy, TPD of CO and the hydrogenation of 1,3-butadiene, a reaction which is sensitive to changes in the electronic density of platinum. The Pt/Al_2O_3 and $Pt–Sn/Al_2O_3$ were used as reference.

[1] Corresponding author; also Escola de Quimica, UFRJ, Rio de Janeiro, Brazil. E-mail: nucat@peq.coppe.ufrj.br.

EXPERIMENTAL

A commercial γ-Al_2O_3 from Harshaw (Al 3996, BET area: 200 m^2/g) and Nb_2O_5 (BET area: 65 m^2/g), obtained by calcination of niobic acid (CBMM, HY 340/AD 929) in air at 773 K for 2 h, were used as supports. The monometallic catalysts were prepared by incipient wetness impregnation of the supports with an aqueous solution of H_2PtCl_6 (Reagen), or $SnCl_2$ (Analar), followed by drying at 393 K for 16 h and calcination in air at 773 K for 2 h (8). The bimetallic catalysts were obtained by re-impregnation of the tin-supported catalysts by an aqueous solution of H_2PtCl_6. Then, they were dried at 393 K for 16 h and calcined in air at 773 K for 2 h. The metal loading was determined by atomic absorption and the results are presented in Table 1.

Chemisorption experiments were performed in a Micromeritics ASAP 2900C surface analyzer. The samples were dried *in situ* with nitrogen at 393 K, reduced in pure hydrogen with a heating rate of 10 K/min up to either 573 or 773 K and then evacuated overnight. The CO adsorption was performed at room temperature and the CO/Pt ratio was determined from the irreversible CO chemisorption.

Samples for infrared spectroscopy were in the form of self-supporting disks and weighed around 25 mg. The cell consisted of a quartz tube with calcium fluoride windows. Viton o-rings provided a gastight seal between removable parts of the cell. The sample analysis was carried out with a Perkin–Elmer model 2000 FTIR in a resolution of 2 cm^{-1}. The catalysts was dried, reduced, and evacuated as described above. CO adsorption was then performed at 298, 323, 353, 383, and 433 K with subsequent evacuation after each adsorption point. The absorbance spectra were obtained by using the interferograms of reduced samples as background references. The CO surface coverage was complete after evacuation at 298 K. The CO coverage at

0021-9517/97 $25.00

TABLE 1

Irreversible CO Chemisorption at 298 K after Reduction at 573 or 773 K

Catalysts	Pt (wt%)	Sn (wt%)	*T* reduction (K)	CO/Pt
Pt/Al_2O_3	1	—	773	0.70
$Pt–Sn/Al_2O_3$	1	1	773	0.55
Pt/Nb_2O_5	1	—	573	0.30
Pt/Nb_2O_5	1	—	773	0.05
$Pt–Sn/Nb_2O_5$ (1 : 1)	1	1	573	0.43
$Pt–Sn/Nb_2O_5$ (1 : 1)	1	1	773	0.26
$Pt–Sn/Nb_2O_5$ (1 : 2)	1	2	573	0.35
$Pt–Sn/Nb_2O_5$ (1 : 2)	1	2	773	0.22

higher temperatures were obtained by dividing the total integrated area of the linearly bonded CO vibration bands at each temperature by the total integrated area obtained after evacuation at room temperature. The statistical variation relating to the number of measurements at various coverage was 3 cm^{-1}.

Temperature programmed desorption (TPD) was performed in a dynamic mode apparatus. The catalyst (typically 0.3–0.5 g) was dried and reduced as described above. After reduction the sample was purged with Argon at either 573 or 773 K until no H_2 was detected in the effluent and then cooled to room temperature. CO was admitted by injecting pulses of 0.08 cm^3 into the argon carrier-gas stream until complete saturation of the catalyst surface was obtained. Desorption was performed by heating the catalysts at 20 K/min from 298 to 823 K in flowing argon. The effluent gas composition was monitored on-line by a quadrupole mass spectrometer (Dycor MA100M-Ametek).

The hydrogenation of 1,3-butadiene was performed in a flow microreactor at atmospheric pressure and at 298 K. The catalyst (ca 50 mg) was mixed with quartz as diluent (100 mg) and then dried with flowing nitrogen at 393 K before reduction with hydrogen at 573 or 773 K. The reaction mixture consisted of 1,3-butadiene/hydrogen/nitrogen (10 : 10 : 80). The reaction conditions were established in order to keep conversion below 12% and there were no transport limitations on the rate. The reaction products were analyzed by an on-line gas chromatograph (VARIAN 2400, with a 80/100 Carbopack C/0, 19% picric acid column at 313 K).

RESULTS

A. Chemisorption and FTIR of Carbon Monoxide

Table 1 presents the results of irreversible CO chemisorption at 298 K. Platinum catalysts supported on alumina exhibited higher CO/Pt ratio than those on niobia, in accordance with our previous works (8, 10). These results are probably associated with the oxychlorinated platinum complexes (PtO_xCl_y) formed on the alumina surface during the calcination (11). However, the less dispersed α-PtO_2 are the predominant species over the niobia surface (10). The partial reduction of Nb_2O_5 could also influence the low CO/Pt ratios.

The addition of tin to Pt/Al_2O_3 resulted in a decrease in the CO/Pt ratio, in agreement to the H/Pt ratio observed elsewhere for $Pt–Sn/Al_2O_3$ catalyst (8). Also, the CO chemisorption decreases on Pt/Nb_2O_5 after reduction at high temperature, which is attributed to the SMSI effect. However, for $Pt–Sn/Nb_2O_5$ catalysts the CO/Pt ratio decreases less after reduction at 773 K. These results suggest a preferential bimetallic effect on $Pt–Sn/Nb_2O_5$, instead of a metal/support interaction, in agreement with previous results observed with Pd–Cu bimetallic systems supported on niobia (12). The different amounts of tin could not promote significant changes in the CO/Pt ratio. The irreversible CO adsorption on Nb_2O_5, Al_2O_3, Sn/Nb_2O_5, and Sn/Al_2O_3 were negligible under the same conditions.

Figures 1–3 present the thermal desorption FTIR spectra of CO adsorbed on the niobia catalysts. The peaks between 2060–2075 cm^{-1} are attributed to the linearly bonded CO on platinum at room temperature. Noteworthy is the peak around 1570–1610 cm^{-1} which, according to Hicks *et al.* (13), can be attributed to formate anions on the support. Negligible amounts of bridge-bonded CO (1780–1860 cm^{-1}) were observed on niobia and $Pt–Sn/Nb_2O_5$ catalysts. The Pt/Nb_2O_5 reduced at 773 K did not exhibit any sensible spectrum, probably due to small amounts of CO adsorbed on this sample.

Figure 4 displays the CO peaks as a function of CO coverage on niobia catalysts. The results were obtained by thermal desorption experiments. The curves were extrapolated for zero surface coverage to determine the vibration frequency of isolated CO molecules. Table 2 shows the results

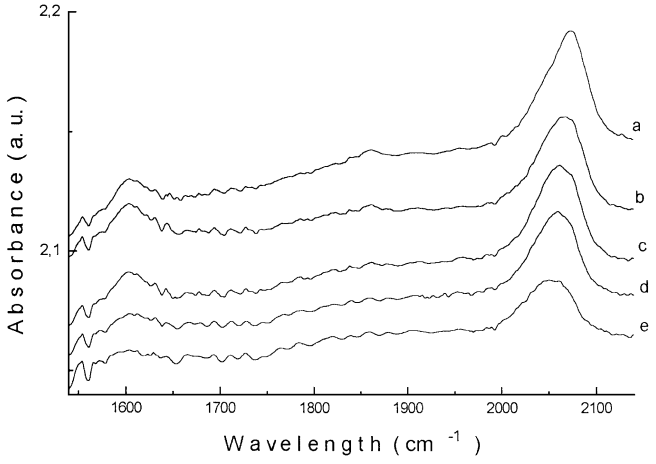

FIG. 1. Thermal desorption infrared spectra of CO for Pt/Nb_2O_5 catalyst reduced at 573 K with spectra obtained at the following desorption temperatures: (a) 298 K, (b) 323 K, (c) 353 K, (d) 383 K, and (e) 423 K.

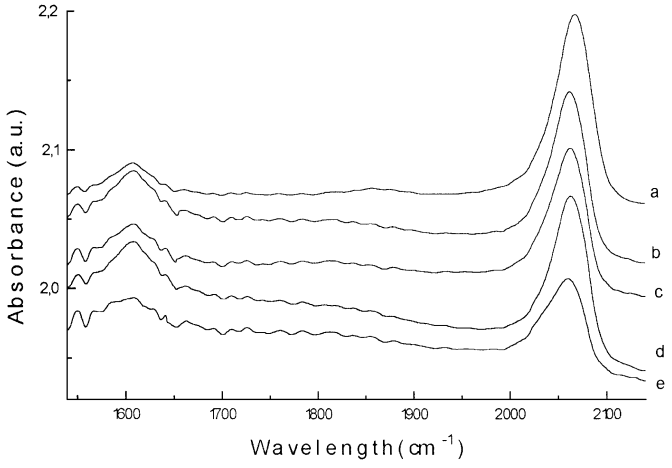

FIG. 2. Thermal desorption infrared spectra of CO for Pt–Sn/Nb_2O_5 (1 : 1) catalyst reduced at 573 K with spectra obtained at the following desorption temperatures: (a) 298 K, (b) 323 K, (c) 353 K, (d) 383 K, and (e) 423 K.

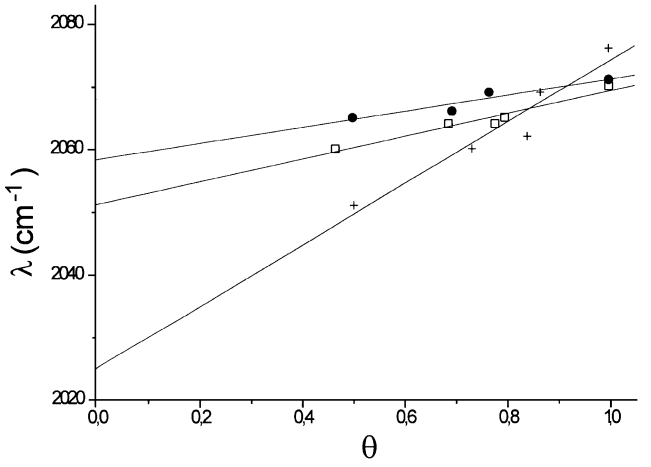

FIG. 4. Infrared peak positions of linearly bonded CO for varying CO surface coverages for niobia supported catalysts. (+) Pt/Nb_2O_5 reduced at 573 K; (□) Pt–Sn/Nb_2O_5 (1 : 1) reduced at 573 K; (●) Pt–Sn/Nb_2O_5 (1 : 1) reduced at 773 K.

of the niobia-supported catalysts, compared to the Pt/Al_2O_3 and Pt–Sn/Al_2O_3 catalysts (14). The different dispersions on Pt/Al_2O_3 and Pt–Sn/Al_2O_3 catalysts do not have significant influence on the singleton vibration frequencies. However, the results are clearly different for niobia-supported catalysts. For Pt/Nb_2O_5 reduced at 573 K the linearly bonded CO vibration frequency decreased drastically. The opposite occurred with Pt–Sn/Nb_2O_5. The singleton vibration frequency increased with the reduction temperature for the bimetallic catalysts supported on niobia.

B. TPD of CO

Figure 5 displays the TPD profiles of CO on Pt/Al_2O_3 and Pt–Sn/Al_2O_3 catalysts. The Pt/Al_2O_3 catalyst exhibits two CO desorption peaks around 490 and 640 K. After reaching 570 K, the CO desorption is accompanied by symmetric profiles of the by-products H_2 and CO_2, which according to Jackson *et al.* (15) are probably ascribed to the dehydroxilation process, or to the decomposition of formate species, according to Hicks *et al.* (13). The desorption profile of CO on Pt–Sn/Al_2O_3 shows one shoulder at low temperature and a second peak at higher temperatures, a feature which was observed also on the Pt/Al_2O_3 profile. However, CO_2 and H_2 are released at lower temperatures on Pt–Sn/Al_2O_3, compared to the Pt/Al_2O_3 catalyst.

The desorption profiles of CO on Pt/Nb_2O_5 catalysts are shown in Fig. 6 for reduction temperatures of 473, 573, and 773 K to evaluate the effect of niobium suboxide on the platinum surface. The CO_2/H_2 release on niobia-supported catalysts occurred at significantly lower temperatures, compared to Pt/Al_2O_3 and Pt–Sn/Al_2O_3 catalysts. After reduction at 473 K, a small amount of CO_2 is formed in the temperature range between 330–440 K. This may be attributed to a subsequent reduction of platinum oxide due to preadsorbed CO molecules on the metallic surface. However, by increasing the reduction temperature,

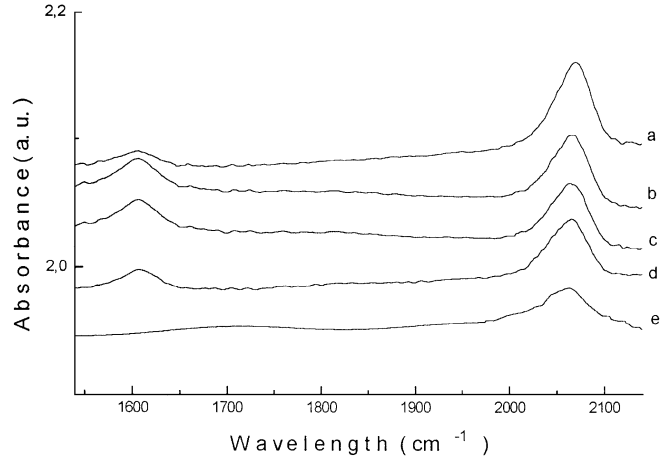

FIG. 3. Thermal desorption infrared spectra of CO for Pt–Sn/Nb_2O_5 (1 : 1) catalyst reduced at 773 K with spectra obtained at the following desorption temperatures: (a) 298 K, (b) 323 K, (c) 353 K, (d) 383 K, and (e) 423 K.

TABLE 2

CO Singleton Vibration Frequency for Platinum Catalysts

Catalysts	*T* reduction (K)	$\lambda\ (\theta = 0)\ cm^{-1}$
Pt/Al_2O_3[a]	773	2045 ± 3
Pt–Sn/Al_2O_3[a]	773	2045 ± 3
Pt/Nb_2O_5	573	2025 ± 3
Pt–Sn/Nb_2O_5 (1 : 1)	573	2052 ± 3
Pt–Sn/Nb_2O_5 (1 : 1)	773	2058 ± 3

[a] Ref. (14).

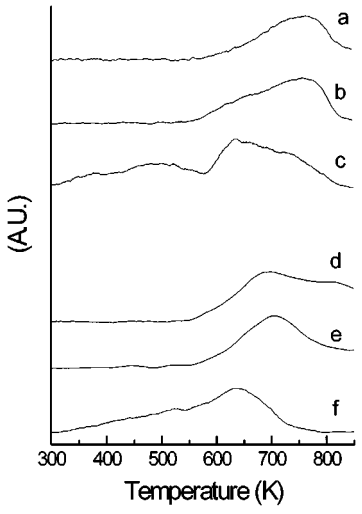

FIG. 5. Desorption profiles, after CO adsorption on Pt/Al_2O_3 reduced at 773 K: (a) H_2, (b) CO_2, (c) CO and $Pt–Sn/Al_2O_3$ reduced at 773 K: (d) H_2, (e) CO_2, and (f) CO.

surprisingly less CO_2 was formed in the presumed dehydroxylation or decomposition region. However, the H_2 released from Pt/Nb_2O_5 catalyst reduced at 773 K indicates that dehydroxylation may occur. To confirm this hypothesis, subsequent chemisorption/TPD cycles were performed. Table 3 presents the results obtained for the Pt/Nb_2O_5 catalyst reduced at 673 K (partial SMSI state).

Results indicate changes on the available metallic surface. After the second TPD, the CO/Pt ratio was 70% higher than in the first chemisorption. Therefore, the available metallic surface area increased after heating with the preadsorbed CO. However, the CO uptake decreases after the third TPD cycle which indicates some deactivation. This phenomenum was less pronounced after reduction at 773 K. The CO chemisorption capacity was very low, probably because at this temperature almost all platinum surface was covered by niobium suboxide species (10).

TABLE 3

Cycles of CO Chemisorption/TPD on Pt/Nb_2O_5 Catalyst Reduced at 673 K

Pt/Nb_2O_5 reduced at 673 K	CO/Pt
1st chemisorption (after reduction)	0.14
2nd chemisorption (after 1st TPD)	0.19
3rd chemisorption (after 2nd TPD)	0.25
4th chemisorption (after 3rd TPD)	0.20

The CO TPD profiles of Pt/Nb_2O_5 reduced at higher temperatures show that the H_2 and CO_2 outputs occur at much lower temperatures. Moreover, the amount by pure CO desorbed was less on these samples than on alumina itself.

Figure 7 displays the TPD profiles of CO for the bimetallic $Pt–Sn/Nb_2O_5$ catalysts. It also indicates a surface reaction with the formation CO_2 and H_2. However, tin substantially promotes the CO desorption from the metallic surface on both catalysts. In these samples the CO output began at 300 K. The effect of tin content on the TPD profiles was negligible.

C. 1,3-Butadiene Hydrogenation

The results of the 1,3-butadiene hydrogenation are presented in Table 4. The turnover frequency decreases with the addition of tin on Pt/Al_2O_3 and this decreasing is more

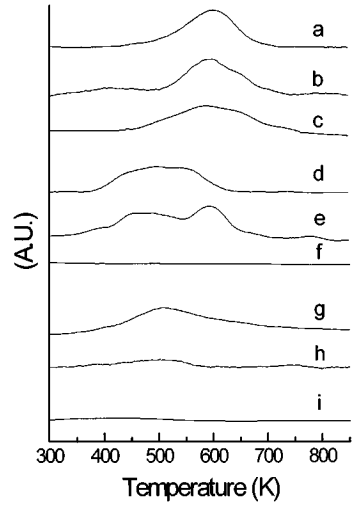

FIG. 6. Desorption profiles, after CO adsorption on Pt/Nb_2O_5 catalysts reduced at 473 K: (a) H_2, (b) CO_2, (c) CO; reduced at 573 K: (d) H_2, (e) CO_2, (f) CO; and reduced at 773 K: (g) H_2, (h) CO_2, and (i) CO.

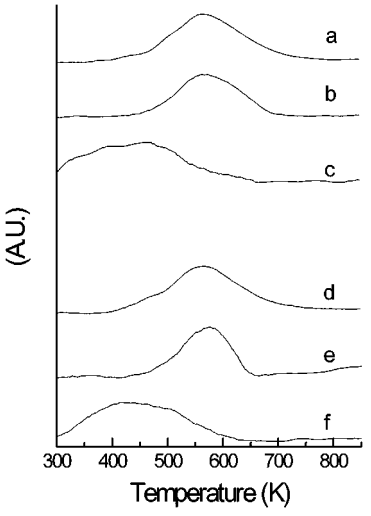

FIG. 7. Desorption profiles, after CO adsorption on $Pt–Sn/Nb_2O_5$ catalysts reduced at 773 K for: $Pt–Sn/Nb_2O_5$ (1:1): (a) H_2, (b) CO_2, (c) CO; and $Pt–Sn/Nb_2O_5$ (1:2): (d) H_2, (e) CO_2, and (f) CO.

TABLE 4

Activity and Selectivity of Platinum Catalysts in 1,3-Butadiene Hydrogenation

Catalysts	*T* reduction (K)	Selectivity (%)			*Trans/cis* 2-butene ratio	TOF (s^{-1})
		Butane	1-Butene	2-Butenes		
Pt/Al_2O_3	773	78	18	4	1.8	66
$Pt–Sn/Al_2O_3$	773	60	30	10	2.7	26
Pt/Nb_2O_5	573	40	40	20	1.4	28
	773	30	45	25	1.6	19
$Pt–Sn/Nb_2O_5$ (1:2)	573	40	40	20	2.0	27
	773	10	80	10	1.5	8

pronounced on niobia-supported catalysts after reduction at higher temperature. Either the bimetallic formation or the SMSI effect has occurred to provoke the decay of the activity. This effect has been explained in other similar systems (12, 16) by the geometric model.

Complete hydrogenation yielding butane was higher on alumina-supported catalysts (over 60–80%) than on niobia-supported catalysts. Unlike the palladium catalysts (12, 16) all platinum systems exhibited lower yield of *trans*- and *cis*-2-butenes. Furthermore, significant differences were not observed in the trans/cis ratio since both the conversions and the yields were low.

The selectivity exhibited sensitivity to the SMSI effect, which is evident upon comparing the Pt/Nb_2O_5 and Pt/Al_2O_3 catalysts. Notwithstanding is that the addition of tin provoked unambiguous changes in the selectivity after the reduction of the $Pt–Sn/Nb_2O_5$ catalysts at 773 K, since the 1-butene formation increases and the complete hydrogenation toward butane decreases fourfold. However, tin in the $Pt–Sn/Al_2O_3$ has a minor effect on the butadiene hydrogenation and practically no effect on the $Pt–Sn/Nb_2O_5$ catalyst reduced at 573 K, compared to the Pt/Nb_2O_5.

DISCUSSION

A. TPD of CO

The interaction of H_2 and CO with group VIII-A metals is a common phenomenon used to identify metallic surfaces. Indeed, since the work presented by Ammenomya and Cvetanovic (17) desorption of probe molecules and, in particular, CO has been used in several studies for morphological analysis of metallic particles (18); estimation of parameters in surface science (19) and alloying and carrier effects in supported metallic and bimetallic catalysts (20).

The reactivity of CO molecules during the TPD is an important point of discussion in the literature. CO_2 is often detected during TPD of CO on supported metal catalysts which has been usually attributed to the disproportionate reaction of CO adsorbed on metal surfaces (21). Hicks *et al.* (13) proposed that adsorbed CO leads to the formation of formate species, which are then decomposed by heating during the TPD experiment. Jackson *et al.* (15) have employed TPD of CO with mass spectrometry to show that during the CO desorption on Pt/Al_2O_3, H_2 and CO_2 are released. This was attributed to a surface reaction between adsorbed CO on the metal and their neighboring hydroxyls on the support. One can describe this reaction as a modified water–gas shift reaction, where the support hydroxyls play the role of water. This symmetric release of CO_2 and H_2 during the TPD of CO was also observed in our work for both alumina and niobia platinum catalysts. Formate species were also detected on the niobia surface by FTIR studies. Figures 1–3 show that after heating the vibration peaks around 1600 cm^{-1} decrease, which is ascribed to formate species. Thus, the decomposition of these surface species due to heating is confirmed. However, the TPD profiles show relatively high intensities of symmetric CO_2 and H_2 release, as compared to CO desorption. Hence, it seems that the amount of CO adsorbed on the metal at room temperature and confirmed by FTIR is not completely released and detected during the TPD. Thus, the reaction of desorbed CO and neighboring hydroxyls of the support, as described elsewhere (15), seems also to play an important role in these systems.

The CO, CO_2, and H_2 profiles of the Pt/Al_2O_3 catalyst were similar to those observed by Jackson *et al.* (15). However, the addition of tin on the Pt/Al_2O_3 catalyst seems to promote the dehydroxilation process which can be attributed to the $Sn^{+2}–Al_2O_3$ interaction described in the literature (22), producing weaker hydroxyl bonds with the alumina vacancies.

The reaction of CO with hydroxyls on the niobia surface is easier than on alumina support, starting at much lower temperatures. The structure of niobia has been studied by infrared spectroscopy and the results have shown that the hydroxyls on niobia are more labile than on alumina surfaces (23). The temperature of reduction and the addition of tin affect the dehydroxylation process induced by CO molecules on niobia supported catalysts. To evaluate these results, additional specific studies are needed concerning the kind of surface structure of niobia.

After a high temperature of reduction of the supported niobia catalysts the chemisorption values decrease sharply, which is known to be due to SMSI effect. The decoration model has been accepted to explain this phenomenon and describes the migration of suboxide species onto the metallic surface and blocking the metal particles (24). Results show that after reduction at 773 K, followed by reoxidation at room temperature, the hydrogen chemisorption capacity was completely restored, indicating that the SMSI effect is also reversible (10). This explains the decrease of CO_2 released after a high temperature of reduction of the

niobia supported catalysts and the significant increase of CO chemisorption after the TPD/chemisorption cycles, suggesting reoxidation of the suboxide niobium species over the metallic surface by CO_2 released during the dehydroxilation process promoted by CO molecules, according the following reactions:

$$CO + OH \rightarrow CO_2 + \tfrac{1}{2}H_2 \qquad \text{(Ref. (15))}$$

$$CO_2 + NbO_x \rightarrow CO + Nb_2O_5 \qquad [1]$$

$$CO_2 + NbO_x \rightarrow C + Nb_2O_5. \qquad [2]$$

Both reactions [1], [2] may occur at the Pt/NbO_x interface. The first is followed by the reaction of CO with hydroxyls, after its regeneration, since no significant CO is released during the TPD of the Pt/Nb_2O_5 catalysts after reduction at high temperatures. The second reaction is more probable and may explain the deactivation process, as observed from the third TPD results presented in Table 2, blocking the active sites. However, sintering may not be discarded after subsequent cycles and this explains the decrease of CO adsorption. Haller *et al.* (25) have already observed that the SMSI can be destroyed by CO_2 during the Fischer–Tropsch synthesis.

The desorption process of CO on $Pt–Sn/Nb_2O_5$ displays similar profiles, but in addition to the CO consumption by the neighboring hydroxyls, it also exhibits desorption of CO at 300 K and during a long period of time, which suggests the presence of different types of metallic sites. This was not observed on Pt/Nb_2O_5. The earlier desorption of CO due to the presence of tin on platinum was discussed by Sachtler *et al.* (20) for Pt–Sn alloys to explain the ligand effect. Therefore, these results indicate the Pt–Sn alloying on supported niobia after reduction at high temperature, in agreement with our previous work (8), and the different adsorption properties of CO at the surface, which is weakly bonded and easily desorbed at the surface after heating. However, the dehydroxylation process was also observed on the $Pt–Sn/Nb_2O_5$ catalysts, which indicates the presence of relatively stronger CO molecules bonded at the surface and capable of reacting only at higher temperatures. It is very important to notice that the SMSI effect observed on Pt/Nb_2O_5 cannot promote the CO desorption. On the contrary, the CO desorption and the dehydroxilation did not occur before 373 K.

B. Infrared of CO

The infrared results show mainly linear adsorption bands of CO on Pt. This implies that the relatively low CO/Pt ratio observed in the chemisorption results for Pt/Nb_2O_5 and $Pt–Sn/Nb_2O_5$ are due to the ensemble effect and the bimetallic formation and are not due to a lower dispersion of platinum particles only. Moreover, IR results confirm the presence of formate anions and also carbonates on both supports (13, 14).

This technique has also been used to identify the geometric and ligand effects on mono and bimetallics catalysts (26–28). Indeed, by extrapolation of the vibration frequency of linearly bonded CO adsorption at zero surface coverage it is possible to explain the CO/metal interaction by excluding the CO intermolecular vibrational coupling (29). For well-dispersed platinum catalysts the extrapolation frequency of linearly adsorbed CO bands were observed around 2040–2050 cm^{-1} (26–28). The results are presented in Table 2 and indicate unambiguous changes in the vibration frequency of CO bonded with Pt and Pt–Sn supported on niobia. The effect of particle size on the CO singleton vibration frequency is not discarded. However, the large differences observed for the frequency values assigned to λ ($\theta = 0$) between niobia-supported catalysts and the usual platinum surfaces indicate a more elaborate phenomenon.

The SMSI effect on titania supported catalysts was also explained through ligand effect (30, 31) although the geometric model has been more evidenced (24). There are only few studies on the mechanisms involving metal/niobia catalysts where ligand effects have been cited (12, 32, 33).

The singleton vibration frequency 2025 cm^{-1} for the CO adsorption on Pt/Nb_2O_5 is the same as that attributed to CO adsorption on platinum which interacts with the support according to Barth *et al.* (26). Unfortunately, with increasing temperature of reduction the sensitivity becomes too low, due to the small amount of CO adsorption and to the absorptive properties of NbO_x species (33).

Indeed, the shift to lower frequencies is related to the decrease of the C–O bond strength, due to the increasing metal-CO back-bonds (26). Therefore, it justifies proposing an electron transfer phenomenon from the partially reduced niobia to platinum particle with the formation of higher electron density.

The $Pt–Sn/Nb_2O_5$ catalysts have also shown alteration in the frequency values λ ($\theta = 0$). Moreover, they increased with the temperature of reduction which can be attributed to a stronger Pt–Sn interaction, probably due to alloy formation (8). These higher singleton vibration frequency values correspond to a weaker interaction between carbon monoxide and platinum, according to the literature (28). Balakrishnan *et al.* (28) indicated that ligand effect between platinum and ionic tin promotes a band shift toward lower frequencies caused by the increasing electronic density of platinum. However, the FTIR results on $Pt–Sn/Nb_2O_5$ may induce another interpretation compared to $Pt–Sn/Al_2O_3$. The Pt–Sn alloying on niobia must be rationalized on the basis of competition for *d* electrons between metal-CO back-bonds and metal–metal bonds (26). This is in rough agreement with the TPD results which explains the CO release at lower temperature and, therefore, the easier CO desorption from the surface of the bimetallic catalysts supported on niobia.

C. 1,3-Butadiene Hydrogenation

1,3-butadiene hydrogenation has also been used to explain the ensemble and ligand effects on metallic surfaces of supported catalysts (12, 16, 34–36). Despite some contradictory results, two general conclusions are proposed: (a) alteration of the turnover frequency due to changes in particle sizes or ensemble effect; and (b) selectivity changes toward complete or incomplete hydrogenation, which is attributed to changes on adsorption strengths between metallic surfaces and hydrocarbons. Thus, with the help of this reaction, ligand effects have been proposed for some bimetallic systems, like Pd–Cr (37) and Pd–Cu (12).

The mechanisms proposed for this reaction (32) are in good agreement with our previous data obtained on palladium based catalysts (12, 16). Boitiaux *et al.* (36) showed that the addition of an electrodonating compound in the reaction mixture, like piperidine, increased the selectivity toward incomplete hydrogenation (olefins) and that the acceptor ligands (containing O, S, and Cl) have an opposite effect, promoting the carbene adsorption, changing the selectivity toward butane, and decreasing the *trans/cis* ratio. This work exhibits changes in the turnover frequencies with the addition of tin, as well as the SMSI effect, thus confirming the ensemble effect which is attributed to the Pt–Sn and Pt–NbO_x interactions on both alumina and niobia surfaces.

The addition of tin on Pt/Al_2O_3 has a minor effect on the selectivity while the niobia supported catalysts exhibit an unambiguous effect on the electron properties of platinum. The higher selectivity toward incomplete hydrogenation (butenes) is a very good indication of an alteration in the electron density of the metal. Hence, the selectivity toward butane decreases sharply upon comparing Pt/Al_2O_3 and Pt/Nb_2O_5 catalysts. This effect is more pronounced with higher temperatures of reduction. Therefore, it suggests an enrichment of the electron density of platinum in the presence of NbO_x species and this interaction yields an inhibition of the carbene adsorption. The *trans/cis* ratio was not significantly changed since the formation of 2-butenes was very low.

The $Pt–Sn/Nb_2O_5$ catalysts reduced at higher temperatures present the lowest degree of butane formation. This confirms our hypothesis that the platinum–tin bonds occur by alloying the metals on niobia support after high temperatures of reduction. According to the literature, Pt–Sn alloys promote large changes in the adsorptive properties of platinum (20) which, therefore, explains the unusual high selectivity toward 1-butene on the $Pt–Sn/Nb_2O_5$ catalyst.

It is noteworthy that the hydrogen chemisorption uptakes on the $Pt–Sn/Nb_2O_5$ (1 : 1) and Pt/Nb_2O_5 catalysts reduced at 573 K are very similar (8). However, after reduction at 773 K they are completely different, which is attributed to the preferential metal–metal interaction, instead of the SMSI effect on niobia support. Moreover, the hydrogen uptake during TPR of the $Pt–Sn/Nb_2O_5$ catalyst at 773 K reveals that at least 70% of tin was present in a zero-valent state. On the other hand, only 28% of Sn^{+4} was reduced to Sn^0 on a $Pt–Sn/Al_2O_3$ catalyst. This larger presence of Sn^0 probably promotes the Pt–Sn alloying on niobia (8).

On the other hand, the turnover frequency change indicates an ensemble effect of the bimetallic species on the $Pt–Sn/Al_2O_3$ and $Pt–Sn/Nb_2O_5$ catalysts (38, 39). Also, the TOF change indicates an ensemble effect on the Pt/Nb_2O_5 catalyst, probably due to the migration of suboxide species after the high temperature of reduction (40, 41). However, the ensemble effect alone cannot explain the selectivity changes on Pt/Nb_2O_5 and $Pt–Sn/Nb_2O_5$ catalysts and therefore, both ensemble and ligand phenomena are needed to completely describe these behaviors on the niobia-supported catalysts.

SUMMARY

The TPD and FTIR results of CO adsorption, together with the 1,3-butadiene hydrogenation, have shown an increase in the electron density of platinum on the Pt/Nb_2O_5 catalysts due to the Pt–NbO_x interaction. The Pt–Sn alloy formation occurs on the niobia carrier after a higher temperature of reduction. Results indicate that tin promotes the electron transfer from Pt 4*d* band through Pt–Sn links (20), changing the electron density of platinum, modifying the adsorption strength between the surface sites and the molecules, in particular hydrocarbons and CO molecules. In addition, the ensemble effect was also observed by means of the TOF results obtained in the hydrogenation of 1,3-butadiene and a lower selectivity toward hydrogenolysis for the *n*-heptane conversion on Pt/Nb_2O_5 and $Pt–Sn/Nb_2O_5$ (9). These associated results indicate that both ensemble and ligand effects play an important role in these catalysts.

Finally, the addition of Sn on Pt/Al_2O_3 exhibits bimetallic cluster formation which can be successfully explained only by the ensemble effect.

ACKNOWLEDGMENTS

This work has been supported by PRONAC (Programa Nacional de Catálise) and FINEP (Financiamento de Estudos e Projetos). The helpful assistance of Mrs. Ruth Leibsohn in the FTIR measurements is greatly acknowledged. Donato A. G. Aranda thanks to FAPERJ (Fundação de Amparo a Pesquisa do Estado do Rio de Janeiro) for financial support.

REFERENCES

1. Sinfelt, J., *Bimetallic Catalysts*, Exxon Mono. Series, Wiley, New York, 1983.
2. Beltramini, J., and Trimm, D. L., *J. Catal.* **31**, 113 (1987).
3. Abrevaya Imai, U.S. Patent 4,608,360 (1986).
4. Cortright, R. D., and Dumesic, J. A., *Appl. Catal.* **129**, 101 (1995).
5. Davis, B. H., *in* "Selectivity in Catalysis" (M. E. Davis and S. L. Suib, Eds.), ACS Symposium Series, Vol. 517, Am. Chem. Soc., Washington, DC, 1993.

6. Gardner, S. D., Hoflund, G. B., and Davidson, M. R., *J. Catal.* **115**, 132 (1989).
7. Llorca, J., Homs, N., Fierro, J. L. G., Sales, J., and Ramirez de la Piscina, P., *J. Catal.* **166**, 44 (1997).
8. Aranda, D. A. G., Noronha, F. B., Passos, F. B., and Schmal, M., *Appl. Catal.* **100**, 77 (1993).
9. Aranda, D. A. G., Passos, F. B., Noronha, F. B., and Schmal, M., *Catal. Today* **16**, 397 (1993).
10. Aranda, D. A. G., Ramos, A. L. D., Passos, F. B., and Schmal, M., *Catal. Today* **28**, 119 (1996).
11. Lietz, G., Lieske, H., Spindler, H., and Volter, J., *J. Catal.* **81**, 8 (1983).
12. Pereira, M. M., Noronha, F. B., and Schmal, M., *Catal. Today* **16**, 407 (1993).
13. Hicks, R. F., Yen, Q. I., and Bell, A. T., *J. Catal.* **89**, 498 (1984).
14. Passos, F. B., Vannice, M. A., and Schmal, M., *J. Catal.* **160**, 106 (1996).
15. Jackson, S. D., Glanville, B. M., Willis, J., McLellan, G. D., Webb, G., Moyes, R. B., Simpson, S., Wells, P. B., and Whyman, R., *J. Catal.* **139**, 207 (1993).
16. Monteiro, R. S., Noronha, F. B., Dieguez, L. C., and Schmal, M., *Appl. Catal.* **131**, 89 (1995).
17. Amenomiya, Y., and Cvetanovic, R. J., *J. Phys. Chem.* **67**, 144 (1963).
18. Rieck, J. S., and Bell, A. T., *J. Catal.* **96**, 88 (1985).
19. Sandoval, M. J., and Bell, A. T., *J. Catal.* **144**, 227 (1993).
20. Sachtler, W. M .H., and Van Santen, R. A., *Adv. Catal.* **26**, 69 (1977).
21. Foger, K., and Anderson, J. R., *Appl. Surf. Sci.* **2**, 335 (1979).
22. Sexton, B. A., Hughes, A. E., and Foger, K., *J. Catal.* **88**, 466 (1984).
23. Sen, B. K., Saha, A.V., and Chatterjee, N., *Mat. Res. Bull.* **16**, 923 (1981).
24. Haller, G. L., and Resasco, R. E., *Adv. Catal.* **36**, 173 (1989).
25. Haller, G. L., Henrich, V. E., McMillan, M., Resasco, D. E., Sadeghi, H. R., and Sakellson, S., *in* "Proceedings, 8th International Congress on Catalysis, Berlin, 1984," Vol. 5, p. 135.
26. Barth, R., Pitchai, R., Anderson, R. L., and Verykios, X. E., *J. Catal.* **116**, 61 (1989).
27. Barth, R., and Ramachadran, A., *J. Catal.* **125**, 467 (1990).
28. Balakrishnan, K., and Schwank, J., *J. Catal.* **138**, 491 (1992).
29. Haaland, D. M., and Williams, F. L., *J. Catal.* **76**, 450 (1982).
30. Chen, B., and White, J. M., *J. Phys. Chem.* **86**, 3534 (1982).
31. Raupp, G. B., and Dumesic, J. A., *J. Phys. Chem.* **88**, 660 (1984).
32. Hoffer, T., Dobos, S., and Guczi, L., *Catal. Today* **16**, 435 (1990).
33. Noronha, F. B., Frety, R., Primet, M., and Schmal, M., *Appl. Catal.* **78**, 125 (1991).
34. Okamoto, Y., Fukino, K., Imanaka, T., and Teranishi, S., *J. Catal.* **74**, 173 (1982).
35. Tardy, B., Noupa, C., Leclercq, C., Bertolini, J. C., Hoareau, A., Treilleux, M., Faure, J. P., and Nihoul, G., *J. Catal.* **129**, 1 (1991).
36. Boitiaux, J. P., Cosyns, J., and Robert, E., *Appl. Catal.* **49**, 235 (1989).
37. Borgna, A., Moraweck, B., Massardier, J., and Renouprez, A. J., *J. Catal.* **128**, 99 (1991).
38. Volter, J., Lietz, G., Uhlemann, M., and Hermann, M., *J. Catal.* **68**, 42 (1981).
39. Afonso, J. C., Aranda, D. A. G., Schmal, M., and Frety, R., *Fuel Proc. Technol.* **42**, 3 (1995).
40. Santos, J., and Dumesic, J. A., *Stud. Surf. Sci. Catal.* **11**, 43 (1982).
41. Ko, C. S., and Gorte, R. J., *J. Catal.* **90**, 5 (1984).